Journal of Virology

Virology | Full-Length Text

Development of reverse genetics system for Guanarito virus: substitution of E1497K in the L protein of Guanarito virus S-26764 strain changes plaque phenotype and growth kinetics

Satoshi Taniguchi,[1,2] Junki Maruyama,[1] Takeshi Saito,[1] Kirsten Littlefield,[3] Rachel A. Reyna,[1] John T. Manning,[1] Cheng Huang,[1] Masayuki Saijo,[2] Slobodan Paessler[1]

AUTHOR AFFILIATIONS See affiliation list on p. 13.

ABSTRACT Guanarito virus (GTOV) is the causative agent of Venezuelan hemorrhagic fever. GTOV belongs to the genus *Mammarenavirus*, family *Arenaviridae* and has been classified as a Category A bioterrorism agent by the United States Centers for Disease Control and Prevention. Despite being a high-priority agent, vaccines and drugs against Venezuelan hemorrhagic fever are not available. GTOV S-26764, isolated from a non-fatal human case, produces an unclear cytopathic effect (CPE) in Vero cells, posing a significant obstacle to research and countermeasure development efforts. Vero cell-adapted GTOV S-26764 generated in this study produced clear CPE and demonstrated rapid growth and high yield in Vero cells compared to the original GTOV S-26764. We developed a reverse genetics system for GTOV to study amino acid changes acquired through Vero cell adaptation and leading to virus phenotype changes. The results demonstrated that E1497K in the L protein was responsible for the production of clear plaques as well as enhanced viral RNA replication and transcription efficiency. Vero cell-adapted GTOV S-26764, capable of generating CPE, will allow researchers to easily perform neutralization assays and anti-drug screening against GTOV. Moreover, the developed reverse genetics system will accelerate vaccine and antiviral drug development.

IMPORTANCE Guanarito virus (GTOV) is a rodent-borne virus. GTOV causes fever, prostration, headache, arthralgia, cough, sore throat, nausea, vomiting, diarrhea, epistaxis, bleeding gums, menorrhagia, and melena in humans. The lethality rate is 23.1% or higher. Vero cell-adapted GTOV S-26764 shows a clear cytopathic effect (CPE), whereas the parental virus shows unclear CPE in Vero cells. We generated a reverse genetics system to rescue recombinant GTOVs and found that E1497K in the L protein was responsible for the formation of clear plaques as well as enhanced viral RNA replication and transcription efficiency. This reverse genetic system will accelerate vaccine and antiviral drug developments, and the findings of this study contribute to the understanding of the function of GTOV L as an RNA polymerase.

KEYWORDS Guanarito virus, reverse genetics, RNA-direct RNA polymerase, L protein, RNA replication and transcription

Guanarito virus (GTOV), an enveloped single-stranded bi-segmented RNA virus, is the causative agent of Venezuelan hemorrhagic fever (VeHF) and has been designated as a Category A bioterrorism agent by the United States (US) Centers for Disease Control and Prevention. The clinical signs and symptoms of VeHF are fever, prostration, headache, arthralgia, cough, sore throat, nausea, vomiting, diarrhea, epistaxis, bleeding gums, menorrhagia, and melena (1, 2). The lethality rate is 23.1% or higher (3). Since the

Editor Rebecca Ellis Dutch, University of Kentucky College of Medicine, Lexington, Kentucky, USA

Address correspondence to Slobodan Paessler, slpaessl@utmb.edu.

The authors declare no conflict of interest.

See the funding table on p. 14.

Received 16 December 2023
Accepted 21 December 2023
Published 30 January 2024

first recognized outbreak in 1989, VeHF cases were continuously reported until 1997 (4). In the past 20 years, clinical and epidemiological studies have not reported any cases of VeHF, leading some to believe that the virus had gone extinct. However, in 2021, a report described 118 suspected VeHF cases, 30.5% (36/118) of which had been confirmed by epidemiological week 42 in 2021, suggesting that VeHF is reemerging as an infectious disease of public health concern (5).

GTOV belongs to the genus *Mammarenavirus*, family *Arenaviridae*, order Bunyavirales (6). The genus mainly consists of two groups based on their origins: one is mainly detected in the African and European continents (Old World arenaviruses), and the other is mainly detected in American continents (New World arenaviruses). GTOV is a member of the clade B New World arenaviruses, which include other human-pathogenic viruses such as Junín virus (JUNV), Machupo virus (MACV), Sabiá virus (SBAV), and Chapare virus (CHAPV). These viruses are etiological agents of Argentine hemorrhagic fever (AHF), Bolivian hemorrhagic fever, "Brazilian hemorrhagic fever (not an official name)," and Chapare hemorrhagic fever, respectively (1, 7). A few prevention and therapeutic methods for AHF and Lassa fever, caused by Lassa virus (LASV), have been studied and developed. Candid#1, the only approved vaccine against AHF, was developed through a cooperative international effort between Argentine and US governments (8). The off-label usage of ribavirin, a purine nucleoside analog, is one of the antiviral therapeutic methods against arenavirus infection (9–11). Transfusion of immune plasma with defined doses of neutralizing antibodies during the prodromal phase of illness has also been used against AHF patients, especially in AHF-endemic areas (12). Recently, the combined administration of ribavirin and favipiravir, a pyrazine derivative, was used to successfully treat an AHF patient (13). However, there are no approved antiviral drugs and vaccines against VeHF.

The GTOV genome comprises two ambisense single-stranded RNA segments designated S and L (14, 15). The S segment, approximately 3.3 kilobases (kb), encodes two proteins, a glycoprotein precursor (GPC), which is cleaved into stable signal peptide, GP1, and GP2, and a nucleoprotein (NP). The L segment, approximately 7.1 kb, encodes a zinc-binding protein (Z) and an L protein (L). These segments utilize an ambisense coding strategy in which the two open reading frames are encoded in opposite transcriptional orientations, terminating in a central intergenic region. Research conducted on other arenaviruses has determined the function of each viral protein; NP and L are required for transcription of the viral gene and viral RNA replication, GPC mediates viral entry into cells, and the Z functions in the regulation of viral RNA synthesis, orchestration of viral assembly and budding, interaction with host cell proteins, and interferon antagonism (16). However, an analysis of these proteins in authentic GTOV is limited.

Although the endemic area of GTOV is limited to six states in Venezuela, GTOV has nine distinct genotypes that differ by 4–17% in their nucleotide sequence and up to 9% in their amino acid sequence of the NP gene (17). Some GTOV strains, such as INH-95551 and CVH-950801, show clear plaques in Vero cells. However, GTOV strain S-26764, isolated from a 9-year-old male non-fatal case in 1997, shows neither clear cytopathic effects (CPEs) nor clear plaques in Vero and Vero E6 cells (Fig. S1) (3). Here, we generated Vero cell-adapted GTOV strain S-26764, which shows clear CPE and plaques in Vero cells, after serial passage. Furthermore, we used reverse genetics to determine which amino acid changes were responsible for these trait changes.

RESULTS

Characterization of Vero cell-adapted GTOV

Vero cells and Vero E6 cells were infected with wild-type GTOV strain S-26764 (wtGTOV) or Vero cell-adapted GTOV, generated by passaging wtGTOV 17 times in Vero cells (wtGTOV-VP17). The plaques of wtGTOV-VP17 were larger and clearer than those of wtGTOV in Vero cells although wtGTOV-VP17 plaques were less clear in Vero E6 cells (Fig. 1A). The wtGTOV-VP17-infected Vero cells showed clear CPE compared with wtGTOV-infected Vero cells (Fig. 1B). The replication kinetics of wtGTOV-VP17 and wtGTOV in

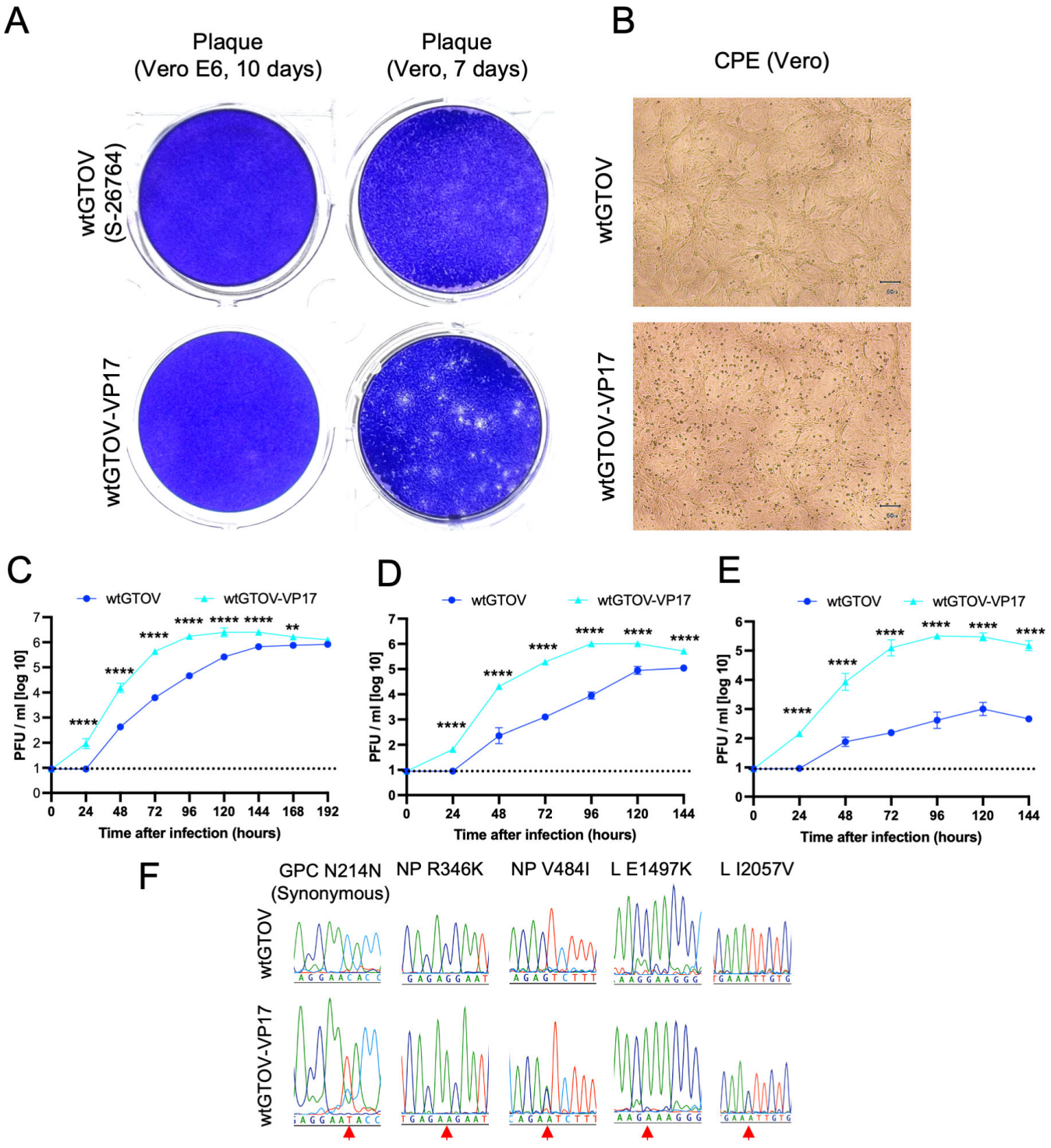

FIG 1 Phenotype characterization of Vero cell-adapted GTOV strain S-26764. (A) Typical plaque morphologies of wild-type GTOV (wtGTOV) and Vero cell-adapted GTOV (wtGTOV-VP17) in Vero and Vero E6 cells. (B) CPE induced by GTOVs. Vero cells were infected with wtGTOV or wtGTOV-VP17 and then observed at 5 days post-infection. Comparison of replication kinetics of wtGTOV and wtGTOV-VP17 in (C) Vero, (D) A549, and (E) Huh7 cells. Results are expressed as the geometric mean viral titer of triplicate experiments. Error bars denote the geometric SD. Statistical analyses were performed using a two-way analysis of variance and Šidák's multiple-comparison test. **** $P < 0.0001$; ** $P \leq 0.01$. Dashed lines indicate the detection limits [<10 plaque-forming units (PFU)/mL]. Experiments shown in panels C–E were performed in triplicate wells for each condition. (F) Sequencing electropherograms at the nucleotide-substituted position. Protein names and amino acid positions corresponding to the substitutions are shown above the electropherograms. Red arrows indicate the substituted nucleotides.

TABLE 1 Nucleic acid difference of viral genome sequence of GTOVs

Gene	Nucleotide position	wtGTOV	wtGTOV-VP11	wtGTOV-VP17	Amino acid change
GPC	642	C	C/T[a]	T[a]	Synonymous
NP	1,037	G	A	A	R346K
NP	1,450	G	G	G/A[a]	V484I
L	4,489	G	A	A	E1497K
L	6,169	A	A/G[a]	A/G[a]	I2057V

[a]Mixed nucleotides determined by Sanger sequencing.

Vero, A549, and Huh7 cells revealed that the growth efficiencies of wtGTOV-VP17 were significantly higher compared with those of wtGTOV in not only Vero cells but also A549 and Huh7 cells (Fig. 1C through E).

Nucleotide mutations in Vero cell-adapted GTOV

The complete genome sequence of wtGTOV was determined to analyze the characteristic changes (GenBank accession numbers LC753262 and LC753263). The complete genome sequence of wtGTOV-VP17 was determined and compared with the wtGTOV genome sequence (Table 1; Fig. 1F). Five nucleotide changes were found in the wtGTOV-VP17 genome sequence compared to that of wtGTOV, resulting in two amino acid changes, R346K and V484I, in NP and two amino acid changes, E1497K and I2057V, in L. The nucleotide mutation in the GPC was a synonymous mutation. The Sanger sequence chromatograms indicated that V484I in NP and I2057V in L were not completely altered, suggesting that there was a mixed viral population. To determine the order of appearance of these nucleotide changes, the genome sequence of wtGTOV-VP11, which was harvested and stored after 11 passages in Vero cells, was determined (Table 1). The results indicated that V484I in NP was acquired after 11 passages. The other alterations were acquired before the 11 passages.

Generation of recombinant GTOV

The recombinant GTOV (rGTOV) was rescued by transfection with murine RNA polymerase I (mPol-I)-driven plasmids encoding S or L segments (pRF-GTOV-SRG and pRF-GTOV-LRG) and polymerase-II-driven NP or L expression plasmids (pC-GTOV-NP and pC-GTOV-L) into BHK-21S cells (Fig. 2A). The viral growth kinetics of recombinant wtGTOV (rwtGTOV) in Vero, Vero E6, A549, and Huh7 cells were compared with those of wtGTOV, indicating that there are no dramatic differences between them (Fig. 2B through E).

Determination of the amino acid responsible for changing the phenotype of GTOVs

The four mutations observed in wtGTOV-VP17 were introduced into pRF-GTOV-SRG and pRF-GTOV-LRG (pRF-GTOV-SRG-NP346K484I and pRF-GTOV-LRG-Lp1497K2057V). Then, recombinant wtGTOV-VP17 (rGTOV-VP17) was rescued. The viral growth kinetics of rGTOV-VP17 in Vero cells did not have dramatic differences with that of wtGTOV-VP17 (Fig. 3A). However, viral yields of rGTOV-VP17 are significantly higher than wtGTOV-VP17 at 4, 5, 6, and 7 days post-infection. To determine the amino acids responsible for the phenotype changes observed in wtGTOV-VP17, recombinant GTOVs possessing one of the four amino acid changes were rescued. rGTOV-NP346K, rGTOV-NP484I, and rGTOV-Lp1497K were successfully rescued, but the rescue of rGTOV-Lp2057V using pRF-GTOV-SRG-Lp2057V was accompanied by the amino acid change of E1497K (rGTOV-Lp1497K2057V). Furthermore, rGTOV-NP346KLp1497K was rescued using pRF-GTOV-SRG-NP346K and pRF-GTOV-LRG-Lp1497K since R346K in NP and E1497K in L were completely altered in wtGTOV-VP17. The plaques of rGTOV-NP484I, rGTOV-Lp1497K, rGTOV-NP346KLp1497K, and rGTOV-VP17 in Vero cells were clearer than those of rwtGTOV, although the plaques of rGTOV-NP346K and rGTOV-Lp1497K2057V in Vero cells were similar to those of rwtGTOV (Fig. 3B). The viral growth kinetics of rGTOVs showed

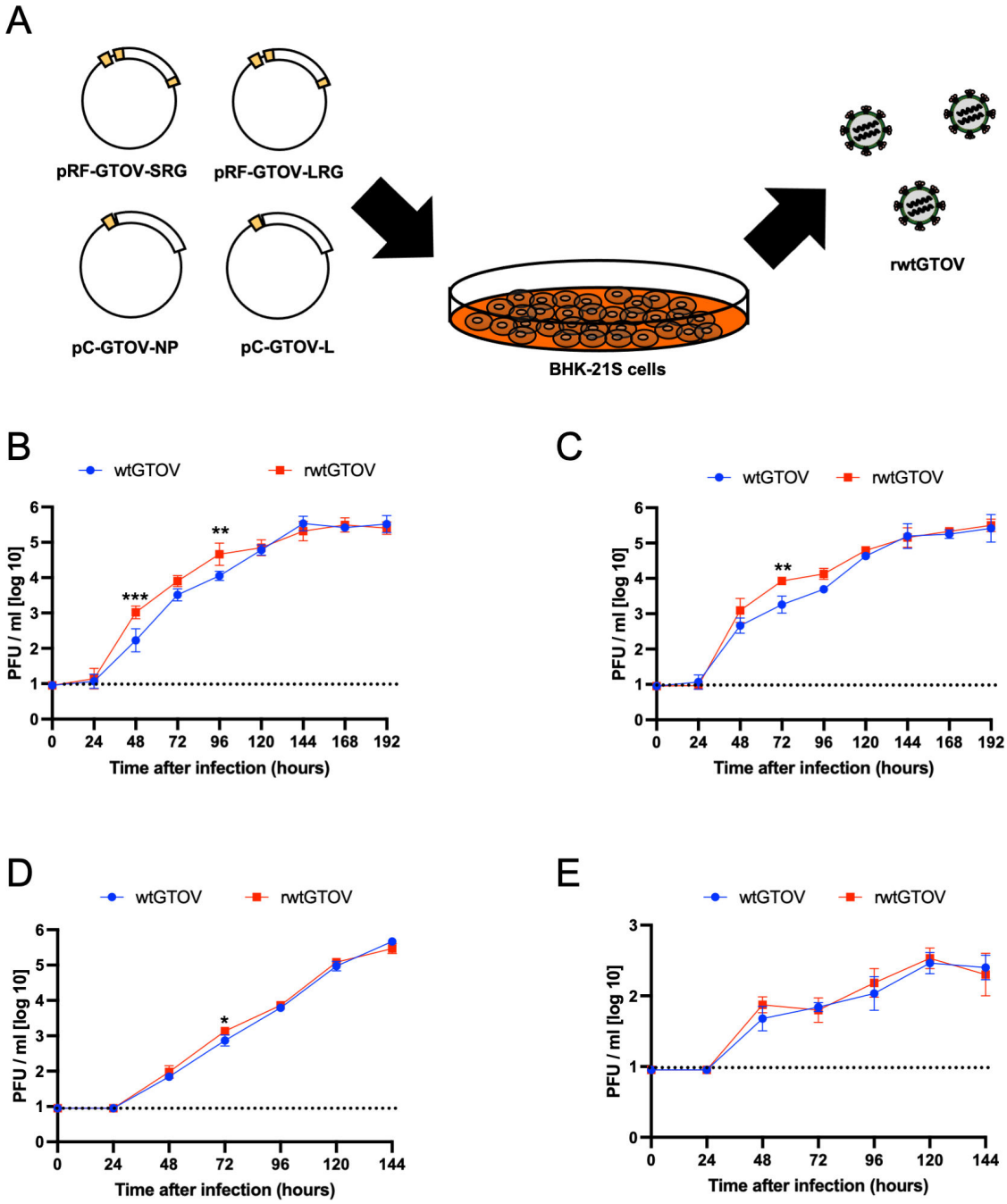

FIG 2 Recombinant GTOV rescued by reverse genetics system. (A) Diagram of the production of recombinant GTOV using a reverse genetics system. BHK-21S cells were transfected with murine RNA polymerase I-driven plasmids to synthesize S and L viral genes and helper plasmids to express NP and L in the cells. Comparison of replication kinetics of wtGTOV and rwtGTOV in (B) Vero, (C) Vero E6, (D) A549, and (E) Huh7 cells. Results are expressed as the geometric mean viral titer of triplicate experiments. Error bars denote the geometric SD. Statistical analyses were performed using a two-way analysis of variance and Šidák's multiple-comparison test. *** $P \leq 0.001$; ** $P \leq 0.01$; * $P \leq 0.05$. Dashed lines indicate the detection limits [<10 plaque-forming unit (PFU)/mL]. Experiments shown in panels B–E were performed in triplicate wells for each condition.

that viral yields of rGTOV-Lp1497K, rGTOV-NP346KLp1497K, and rGTOV-VP17 at 6–8 days post-infection reached 10^6 plaque-forming units (PFU), although those of the other rGTOVs were under 10^6 PFU (Fig. 3C). The viral yields of rGTOV-Lp1497K, rGTOV-NP346KLp1497K, and rGTOV-VP17 at 8 days post-infection were significantly higher than those of rwtGTOV. These results suggested that E1497K in L affects viral replication efficiency. On the other hand, the viral titers of rGTOV-Lp1497K at 1–5 days post-infection

were not significantly higher than those of rwtGTOV, suggesting that not only E1497K substitution in L but also the other substituted amino acids were involved in the rapid growth of wtGTOV-VP17. Additionally, the results suggested that I2057V in L counteracted the effect of E1497K substitution in L.

Comparison of the gene replication efficiency of rGTOVs

To examine the impacts of mutations in NP or L on viral replication efficiency, viral RNA replication levels in infected cells at 24 h post-infection were compared between generated rGTOVs (Fig. 4). Viral RNA loads in cells infected with rGTOV-Lp1497K and rGTOV-NP346KLp1497K were significantly higher than those infected with rwtGTOV, rGTOV-NP346K, rGTOV-NP484I, or rGTOV-Lp1497K2057V. The viral RNA level of rGTOV-VP17 was slightly higher than those of rwtGTOV, rGTOV-NP346K, rGTOV-NP484I, and rGTOV-Lp1497K2057V, but there were no significant differences.

Evaluation of the impact of E1497K substitution in L on viral RNA replication and transcription efficiency

To evaluate the impact of E1497K substitution in L on viral RNA replication and transcription efficiency in Vero cells, a Simian RNA polymerase I (sPol-I)-driven S segment minigenome plasmid (sPol-I-GTOV-SMG) was constructed, and minigenome assay was performed (Fig. 5A). The expression of Firefly luciferase (Fluc) was significantly higher in Vero cells co-transfected with sPol-I-GTOV-SMG and both pC-GTOV-NP and pC-GTOV-L (Fig. 5B). High luciferase expression was detected under the expression of L with E1497K (Fig. 5C). The expression of luciferase was suppressed under the expression of L with E1497K and I2057V.

DISCUSSION

Passaging a virus in various cell lines is one of the classical methods for generating attenuated vaccine candidates and studying viral pathogenicity and characteristics (18–25). JUNV Candid#1, the only approved vaccine against AHF, was developed through serial passage in guinea pigs, mouse brains, and fetal rhesus monkey lung cells (18). In this study, serial passage of GTOV strain S-26764 in Vero cells resulted in several phenotype changes, including plaque morphology, CPE, and viral growth in various cell lines. wtGTOV requires 10 days to form plaques, which are more visible in Vero E6 than in Vero cells. However, even in Vero E6 cells, the plaques are unclear and vague. In contrast, wtGTOV-VP17 takes only 7 days to form plaques in Vero cells, and its plaques are clear, suggesting that wtGTOV-VP17 has enhanced utility for the research with GTOV, such as neutralization assays, drug screening, and plaque reduction assays. Additionally, the rapid growth and high yield of wtGTOV-VP17 are advantageous for use in multiple applications, such as vaccine production. The rapid growth and high yield of wtGTOV-VP17 could be observed in not only Vero cells but also A549 cells and Huh7 cells, suggesting the possibility that the acquired phenotypic changes work cooperatively with primate-derived cell lines. The growth kinetics of wtGTOV-VP17 in rodent-derived cell lines was not investigated in this study. Further investigation to analyze the susceptibility of cell lines derived from other mammalian species, especially rodents, to infection with wtGTOV-VP17 is required to confirm this hypothesis.

To date, reverse genetics systems exist to rescue recombinant LASV, JUNV, and MACV (26–29). Both mPol-I- and T7 RNA polymerase-driven reverse genetics systems were reported for LASV and JUNV. The MACV reverse genetics system, however, is driven by mPol-I. These reverse genetics systems are used for the analysis of pathogenicity, mechanisms of attenuation, protein function, and assessment of vaccine candidates. An mPol-I-driven reverse genetics system for GTOV was newly established in this study, enabling us to introduce arbitrary mutations to GTOV genes and to conduct studies previously performed for LASV, JUNV, and MACV. In addition, an sPol-I-driven minigenome assay was established in this study, providing a high-throughput anti-viral drug screening system for evaluating viral replication inhibitors.

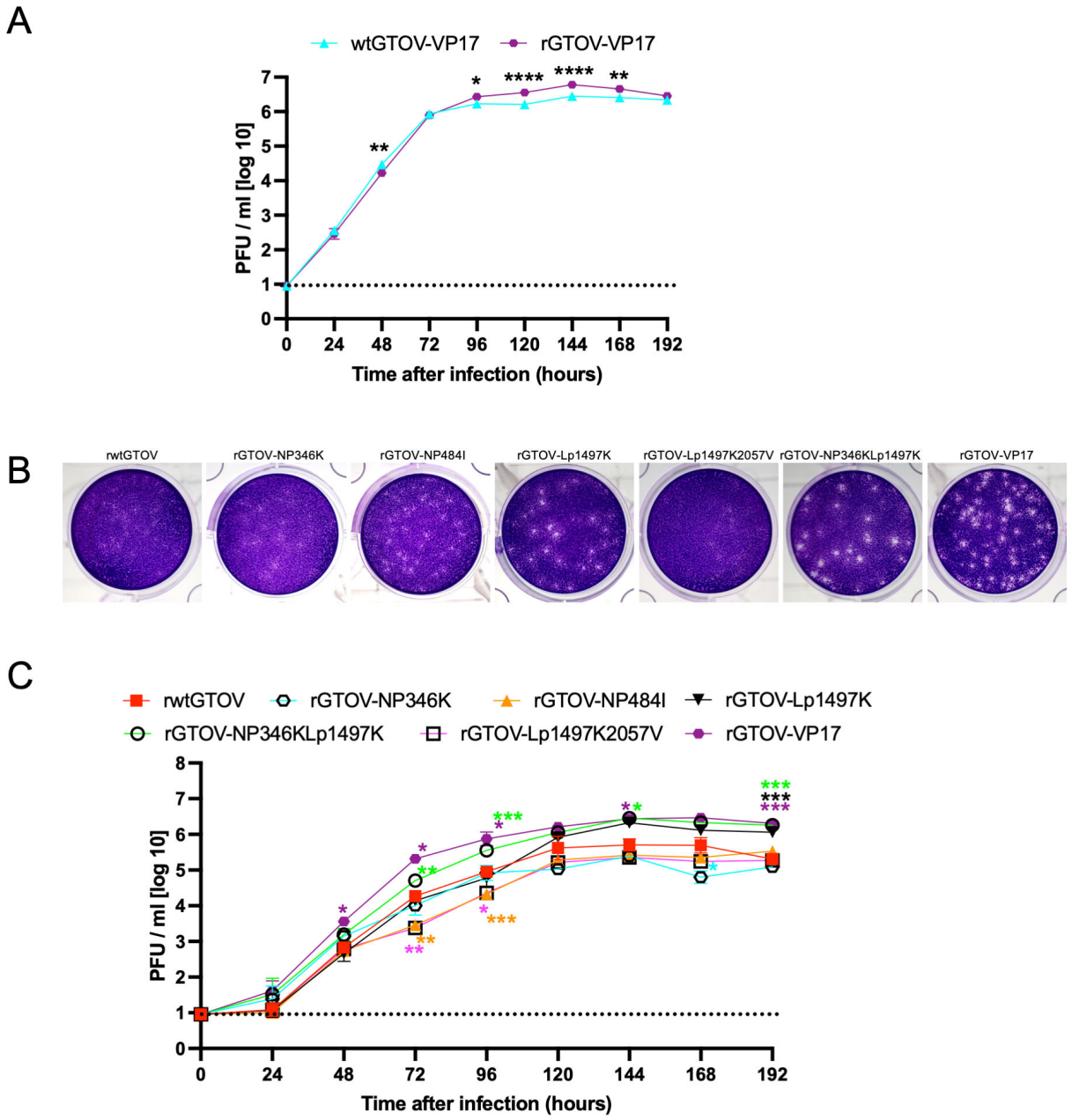

FIG 3 Determination of the amino acid responsible for phenotype changes of GTOV. (A) Comparison of replication kinetics of wtGTOV-VP17 and rGTOV-VP17 in Vero cells. (B) Comparison of plaque morphologies of generated recombinant GTOVs in Vero cells. (C) Comparison of replication kinetics of generated recombinant GTOVs in Vero cells. Results are expressed as the geometric mean viral titer of triplicate experiments. Error bars denote the geometric SD. Statistical analyses were performed using a two-way analysis of variance followed by Šidák's multiple-comparison test in panel A and Dunnett's multiple-comparison test in panel C. The common logarithm viral titers of rGTOVs at each time point were compared to those of rwtGTOV at each time point in panel C. The color of each asterisk is identical to the color of the graph line of the corresponding virus. **** $P < 0.0001$; *** $P \leq 0.001$; ** $P \leq 0.01$; * $P \leq 0.05$. Dashed lines indicate the detection limits (<10 PFU/mL). Experiments shown in panels A and C were performed in triplicate wells for each condition.

wtGTOV-VP17 has four amino acid changes compared to wtGTOV. Two were found in NP and the other two were found in the L. As of November 25, 2023, 30 GTOV full S segment sequences, including LC753262, were registered in GenBank (Table S1). Only two sequences (AY572554 and KR260726) have arginine at the 346th amino acid position in NP, and the other sequences have lysine at this position, suggesting two possibilities: R346K mutation is not specifically acquired via Vero cell adaptation or has happened in

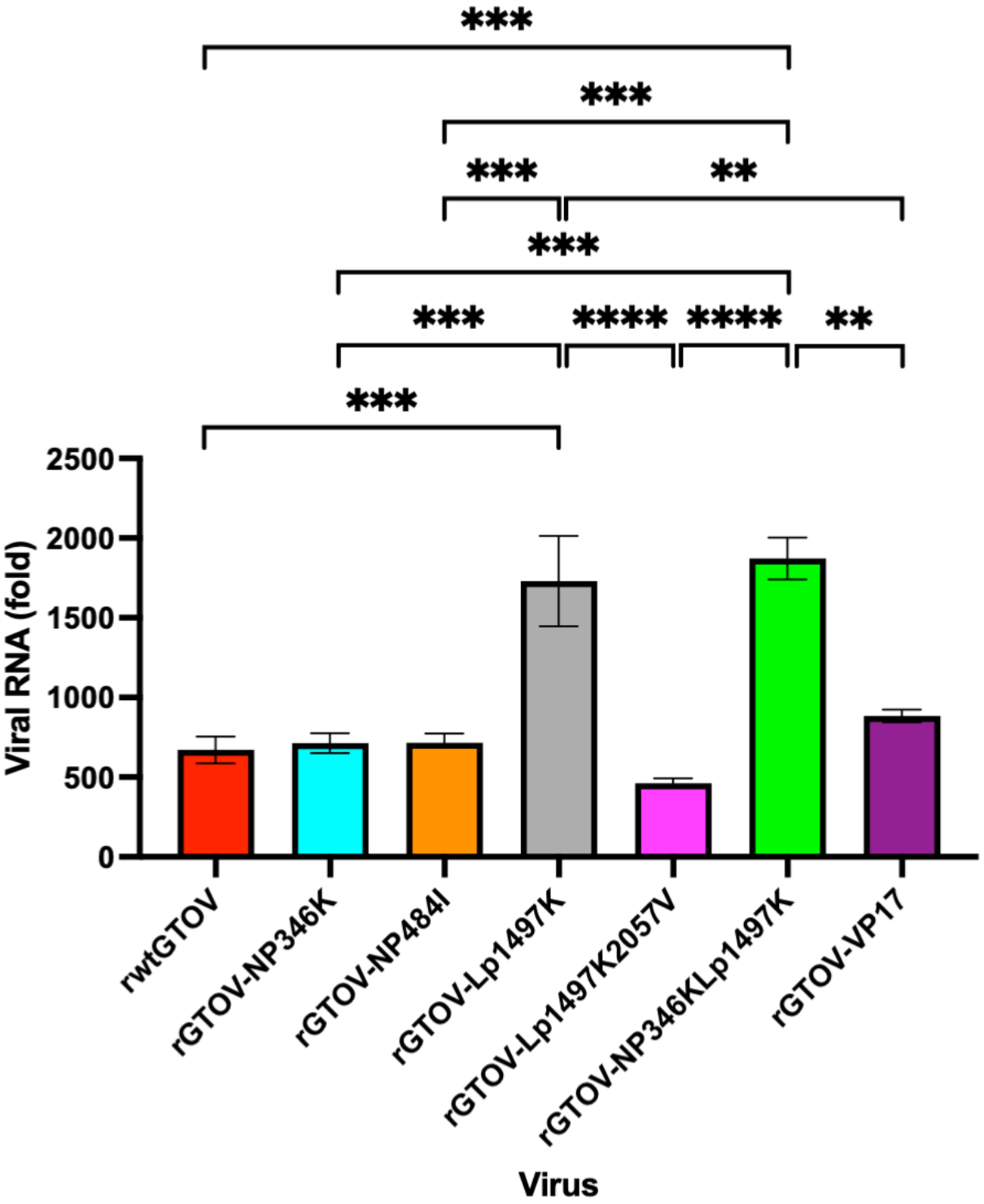

FIG 4 Comparison of rGTOV viral RNA replication levels in infected cells at 24 h post-infection. Vero cells were infected with each rGTOV at a multiplicity of infection of 0.001. Total RNA was extracted from infected Vero cells at 0 or 24 h post-infection. Then, viral RNA levels were quantified by quantitative reverse transcription PCR (qRT-PCR). Results were shown in fold change of viral RNA compared to those at 0 h post-infection. Error bars represent the SEM. Statistical differences were analyzed using a one-way analysis of variance and Tukey's multiple-comparison test. **** $P < 0.0001$; *** $P \leq 0.001$; ** $P \leq 0.01$. All non-remarks between bars indicate $P > 0.05$. The experiment was performed in triplicate wells ($n = 3$) for each virus.

most of GTOVs through virus isolation. Ten out of 30 GTOV S segments registered in GenBank have valine at the 484th amino acid position in NP; the other sequences have isoleucine. There were no obvious differences in isolation sources (human patient

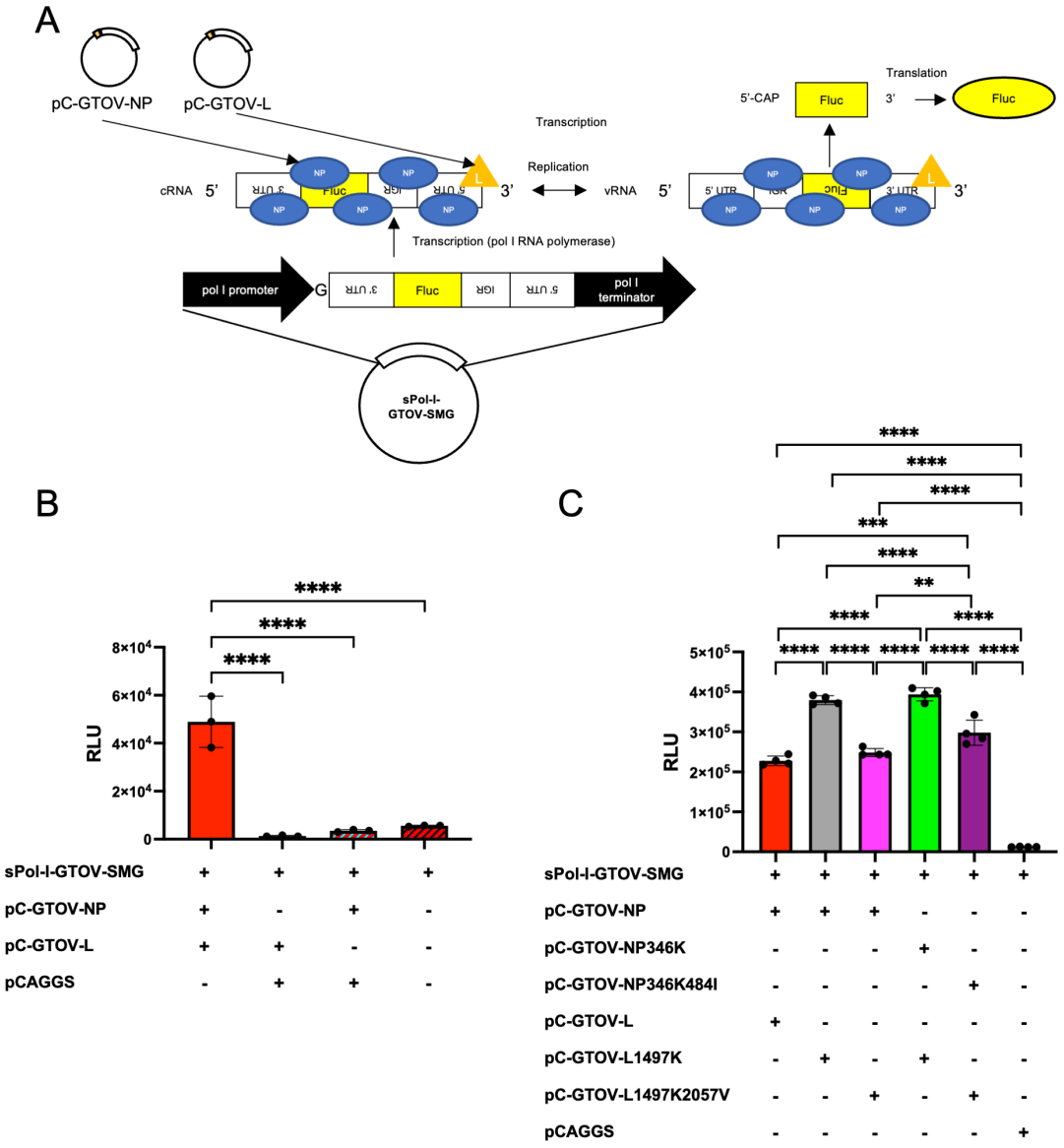

FIG 5 Evaluation of the impact of E1497K substitution in L on viral RNA replication and transcription efficiency. (A) A diagram of the GTOV S segment minigenome plasmid (sPol-I-GTOV-SMG) and its replication, transcription, and translation mechanisms. The cDNA fragment containing the S 3′-untranslated region (UTR), Firefly luciferase (Fluc) open reading frame, intergenic region (IGR), and the S 5′-UTR in the anti-genomic sense is inserted between the simian RNA polymerase I (sPol-I) promoter and murine RNA polymerase I terminator. An additional deoxyguanosine is inserted between promoter and the S 3′-UTR. sPol-I-GTOV-SMG plasmid is transcribed using RNA polymerase I to generate cRNA in Vero cells. The cRNAs are encapsidated with the NP. The vRNAs are produced in the presence of L. The encapsidated vRNA is transcribed into a reporter-gene mRNA. Finally, the transcribed mRNA is translated by the host to produce Fluc. (B) Development of sPol-I-mediated GTOV minigenome system. Vero cells were transfected with sPol-I-GTOV-SMG and pC-GTOV-NP or pCAGGS, pC-GTOV-L, or pCAGGS, and pRL-SV40. Transfected cells were incubated for 2 days at 37°C. Fluc and Renilla luciferase (Rluc) activities were measured, and the RLUs were determined. (C) Comparison of reporter expression levels of minigenomes using mutated NP and L. Vero cells were transfected with sPol-I-GTOV-SMG and pC-GTOV-NP or mutated pC-GTOV-NP, pC-GTOV-L, mutated pC-GTOV-L, or pCAGGS, and pRL-SV40. Transfected cells were incubated for 2 days at 37°C. Fluc and Rluc activities were measured, and the RLUs were determined. Error bars in panels (B) and (C) represent the SD. Statistical differences were analyzed using a one-way analysis of variance and Tukey's multiple-comparison test. ****, $P < 0.0001$; ***, $P \leq 0.001$; **, $P \leq 0.01$. All non-remarks between bars indicate $P > 0.05$. The experiment shown in panel B was performed in triplicate. The experiment shown in panel C was performed in quadruplicate.

samples or rodent samples) between strains that have valine or isoleucine at the 484th amino acid position in NP. Although all other New World arenaviruses (SBAV: JN801474, CHAPV: EU260463, JUNV: AY358023, MACV: JN794584) have lysine at the identical amino acid position of GTOV NP 346th amino acid, the amino acid at the identical position of

GTOV NP 484th amino acid varied (lysine, asparagine, glutamine, and leucine, respectively). These facts suggested that the characteristics of the 484th amino acid are not required to be rigid for arenaviruses, supporting the fact that the 484th amino acid change occurred after 11 passages and was not completely altered through the serial passage in Vero cells.

Nineteen GTOV full L segment sequences, including LC753263, were available at GenBank (Table S2). Two sequences (KU059748 and KU746274) have arginine and 16 sequences have lysine at the 1,497th amino acid in L. wtGTOV used in this study has glutamic acid at this position, whereas SBAV (JN801475), CHAPV (EU260464), JUNV (AY358022), and MACV (JN794583) have lysine, asparagine, arginine, and arginine, respectively. The results of plaque morphology comparison and growth kinetics analysis suggested that E1497K mutation in the L protein had a significant role in making clear plaques and enhancing viral propagation efficiency. GTOV INH-95551 and CVH-950801, which show clear plaques in Vero cells, have lysines at the 1,497th amino acid in L, supporting our hypothesis. Results of the minigenome assay and comparison of viral gene loads in infected cells suggested that E1497K enhanced viral gene replication efficiency. The protein structure of GTOV L remains to be clarified. However, cryo-EM structures of LASV, MACV, and JUNV L proteins were recently reported (30–32). These studies revealed detailed predicted functional domains for the arenavirus L protein. E1497K observed in wtGTOV-VP17 is speculated to be located on the thumb domain of the RNA-direct RNA polymerase (RdRp) region. Considering that the thumb domain is one of the active sites of RNA synthesis, the E1497K mutation may enhance the efficiency of RdRp taking RNA into its catalytic site, affect the binding stability of RNA and RdRp, or enhance the efficiency of polymerase activity.

An I2057V mutation was also found in wtGTOV-VP17 although this mutation is not completely altered. All GTOV full L segment sequences available at GenBank have isoleucine at the 2,057th position of L, while SBAV, CHAPV, JUNV, and MACV have a leucine at the corresponding position, suggesting that the I2057V mutation observed in the present study is unique. Interestingly, introducing this mutation required E1497K mutation in L, and I2057V counteracted the phenotype changes caused by E1497K mutation: I2057V made plaques unclear and reduced viral genome replication efficiency. The slightly higher yields of rGTOV-VP17 than wtGTOV-VP17 in Vero cells supported this hypothesis. The advantage of this mutation is unknown and further examination is required.

In summary, we have passaged GTOV in Vero cells and generated wtGTOV-VP17, which had a high yield and showed clear CPE and plaques in Vero cells. Four amino acid changes were found in wtGTOV-VP17. We have developed the reverse genetics system for GTOV and have analyzed the impact of these amino acid changes on viral characteristics. The results demonstrated that E1497K in L was the key amino acid contributing to the wtGTOV-VP17 phenotype changes affecting plaque phenotype and viral replication efficiency. Vero cells are used for vaccine production (33). Introducing an E1497K substitution in the L of GTOV enhances its yield in Vero cells and clarifies its plaque morphology in Vero cells, suggesting that this substitution gives an advantage to developing vaccine strains. Further studies using the GTOV reverse genetics system established in this study would aid in the development of vaccines and the analysis of GTOV pathogenesis.

MATERIALS AND METHODS

Cells and viruses

Vero, Vero E6, and A549 cells were purchased from the American Type Culture Collection. Huh7 cells were purchased from the Japanese Collection of Research Bioresources. These cells were cultured in the Dulbecco's modified Eagle's medium (DMEM) (Corning, Manassas, VA) supplemented with 10% heat-inactivated fetal bovine serum (FBS) (Gibco,

Paisley, UK) and 100 U/mL of penicillin–streptomycin (HyClone, South Logan, UT) at 37°C in 5% CO_2. BHK-21S cells were maintained with DMEM supplemented with 5% FBS, 10% tryptose phosphate broth (Gibco), and 100 U/mL of penicillin–streptomycin, and cultured at 37°C in 5% CO_2 (34).

GTOV strain S-26764 (provided by Thomas G. Ksiazek, University of Texas Medical Branch, Galveston, TX) was passaged in Vero E6 cells, and viral sequences were determined as described below. This GTOV strain S-26764 served as wtGTOV.

Serial virus passage in Vero cells

Vero cells, cultured in a T-25 flask, were infected with the virus at a multiplicity of infection (MOI) of 0.005 and incubated at 37°C in 5% CO_2 for 4–7 days. The supernatant was harvested, and new Vero cells were infected with 20 µL of the virus-containing supernatant in a T-25 flask with 5 mL of DMEM supplemented with 2% FBS (DMEM-2FBS). Serial passages in Vero cells were performed 17 times.

Plasmids

To construct the plasmids designated pRF-GTOV-SRG and pRF-GTOV-LRG, cDNA fragments containing complete S or L segments of GTOV were cloned between the sequences encoding the mPol-I promoter and the terminator of the pRF vector (29). An additional G residue, which has been reported to enhance the efficiency of virus rescue by reverse genetics, was inserted between the mPol-I promoter and the viral genome sequences (35). Viral cDNA constructs were inserted in the antigenomic sense orientation of the viral RNA. The pRF-GTOV-SRG and pRF-GTOV-LRG plasmids with mutations in the NP or L genes (pRF-GTOV-SRG-NP346K, pRF-GTOV-SRG-NP484I, pRF-GTOV-SRG-NP346K484I, pRF-GTOV-LRG-Lp1497K, pRF-GTOV-LRG-Lp2057V, and pRF-GTOV-LRG-Lp1497K2057V) were generated via site-directed mutagenesis and an in-fusion high-fidelity (HD) restriction-free cloning method (TaKaRa Bio, Shiga, Japan). Plasmids for the expression of GTOV NP and GTOV L (referred to as pC-GTOV-NP and pC-GTOV-L, respectively) were constructed by cloning PCR amplicons of the GTOV NP or GTOV L genes into pCAGGS plasmids linearized by EcoRI/XhoI or EcoRI/NheI using an in-fusion HD restriction-free cloning method. Plasmids for the expression of mutated GTOV NP and L (pC-GTOV-NP346K, pC-GTOV-NP346K484I, pC-GTOV-L1497K, and pC-GTOV-L1497K2057V), which have amino acid substitutions at a designated amino acid number, were constructed with the same cloning strategy as non-mutated pC-GTOV-NP and pC-GTOV-L. To eliminate the difference in protein expression levels in transfected cells between mutated plasmids, all mutated NP or L expression plasmids have the same sequences in non-open reading frame regions with original NP or L expression plasmids. sPol-I-GTOV-SMG was generated from pRF-GTOV-SRG. Briefly, the NP gene was substituted for a Firefly luciferase (Fluc) gene, and the GPC gene was removed. Then, the mPol-I promoter was substituted for sPol-I promoter. A plasmid expressing Renilla luciferase (Rluc) (referred to as pRL-SV40) was purchased from Promega (Fitchburg, WI).

Viral genome sequencing

Viral genome sequences of GTOVs used here were analyzed using Sanger sequencing of cDNAs generated using reverse transcription-PCR (RT-PCR). Total RNA was extracted from infected Vero cells and used. To determine the 5' and 3' termini of the viral genome sequence, a 5' RACE system (Thermo Fisher Scientific, Carlsbad, CA) was used. Briefly, cDNAs were synthesized from RNAs using gene-specific primers and tailed with homopolymeric dCTP. Then, cDNAs were treated with terminal deoxynucleotidyl transferase and subjected to PCRs with gene-specific primers, abridged anchor primer, and universal amplification primer. All these PCR products were purified, and their nucleic sequences were analyzed by Sanger sequencing (36).

TABLE 2 List of real-time PCR primers used in this study

Primer name	Sequence	Target
GTOV S 1620F	TGC ACT CTT GGC TTG GAA CA	GTOV S
GTOV S 1751R	AAC TCC ACA AAG GAA CCG CA	GTOV S

Rescue of recombinant GTOVs

One milliliter of BHK-21S cells (6.0×10^4 /mL) were seeded into wells of 12-well plate 1 day before transfection. Cells were transfected using 6.0 µL of FuGENE HD transfection reagent with 0.4 µg of pRF-GTOV-SRG (or mutated pRF-GTOV-SRG; pRF-GTOV-SRG-NP346K, pRF-GTOV-SRG-NP484I, and pRF-GTOV-SRG-NP346K484I), 0.6 µg pRF-GTOV-LRG (or mutated pRF-GTOV-LRG; pRF-GTOV-LRG-Lp1497K, pRF-GTOV-LRG-Lp2057V, and pRF-GTOV-LRG-Lp1497K2057V), 0.4 µg of pC-GTOV-NP, and 0.6 µg of pC-GTOV-L. Cells were incubated for 4–5 days. The medium used for culturing transfected BHK-21S cells was harvested and stored. Vero E6 cells were inoculated with the medium for 5–6 days, and the supernatants were harvested and stored at −80°C. After viral propagation was confirmed using plaque assay, the RNA of each recombinant virus was extracted, and the viral genome sequences of all recombinant viruses were confirmed using Sanger sequencing (36). The rwtGTOV supernatant was further passaged in Vero E6 cells for 5–6 days, harvested, and used, due to the low yield of the first passaged stocks.

Plaque assay

The virus titer of GTOV was determined as described below. Briefly, after 30-min adsorption of viral inoculum to Vero cells or Vero E6 cells cultured in 12-well plates, cells were overlaid with 1 mL of overlay medium [Eagle's minimum essential medium (MEM) containing 1% Avicel RC-591 NF, 100 U/mL penicillin–streptomycin, and 2–5% FBS] and further cultured for 7 or 10 days at 37°C. The cell monolayers were then fixed with 10% formalin in phosphate-buffered saline, stained using crystal violet, washed with tap water, and dried.

Comparison of viral growth kinetics

All samples for viral growth kinetics experiments were collected as described below. Briefly, 2.0×10^5 Vero, Vero E6, A549, and Huh7 cells were seeded into wells of 12-well plates 1 day before virus infection. Cells were infected with each virus at an MOI of 0.001 and washed three times with DMEM-2FBS after a 30-min adsorption period at 37°C, and 1 mL of DMEM-2FBS was added to each well. Supernatant samples were collected at 0–6 or 0–8 days post-infection. The supernatants were centrifuged at $8,000 \times g$ for 5 min to remove cell debris and were stored at −80°C until the virus titer was measured using a plaque assay.

Quantitative RT-PCR (qRT-PCR) analysis of viral gene expression levels

Vero cells of 2.0×10^5 were seeded into wells of 12-well plates 1 day before virus infection. Cells were infected with each virus at an MOI of 0.001 and washed three times with DMEM-2FBS after a 30-min adsorption period at 37°C, and 1 mL of DMEM-2FBS was added to each well. The supernatant was removed at 0 or 24 h post-infection, and cells were treated with 1 mL of TRIzol reagent (Thermo Fisher Scientific). Total RNA extracted from infected Vero cells was purified with an RNeasy mini kit (QIAGEN, Germantown, MD) after DNase treatment with RNase-Free DNase Set (QIAGEN). RNA was reverse transcribed using SuperScript IV First-Strand Synthesis System (Thermo Fisher Scientific). SsoAdvanced Universal SYBR Green Supermix (Bio-Rad, Hercules, CA) and a CFX96 Touch Real-Time PCR Detection System (Bio-Rad) were used for qRT-PCR with the GTOV primers listed in Table 2. For primers targeting at actin gene, PrimePCR SYBR Green Assay: ACTB, Human (Bio-Rad) was used. The relative RNA levels of the viral genes were

analyzed using the threshold cycle ($2^{-\Delta\Delta CT}$) method using qRT-PCR (37). The CT of β-actin was used as the internal reference.

Simian RNA polymerase I-driven minigenome assay

The minigenome assay was carried out with modification from a previously reported mPol-I-driven minigenome method (38). Briefly, 5.0×10^4 Vero cells were seeded into wells of 24-well plates 1 day before transfection. Cells were transfected with minigenome plasmids (0.24 µg of sPol-I-GTOV-SMG), 0.24 µg of NP expression vector or pCAGGS vector (empty vector), 1.0 µg of L expression vector or empty vector, and 0.01 µg of pRL-SV40; transfections were conducted using VeroFect transfection reagent (OZ Biosciences, San Diego, CA). The total amount of DNA used in transfections was maintained at 1.49 µg, and the amount of transfection reagent was maintained at a constant ratio of three volumes (µL) per amount of DNA added (µg). Transfected cells were incubated for 2 days at 37°C. Fluc and Rluc activities were measured using a Dual-Luciferase Assay System (Promega). The luminescence level was measured, and the relative luminescence units (RLUs) of luciferase were determined using a GloMax 96 luminometer (Promega). All results obtained for Fluc were normalized to the expression levels of Rluc.

Statistical analyses

All bar graphs were drawn using GraphPad Prism 9 software (GraphPad Software, Inc.) and statistically analyzed using a one-way analysis of variance (ANOVA) and Tukey's multiple-comparison test to analyze the RLU levels or viral RNA levels. Virus growth curves were generated using GraphPad Prism 9 software. All viral growth curves except for Fig. 3C were analyzed using a two-way ANOVA and Šidák's multiple-comparison test to analyze the common logarithm of viral titers. The viral growth curves of Fig. 3C were analyzed using a two-way ANOVA and Dunnett's multiple-comparison test. The common logarithm viral titers of rGTOVs at each time point were compared to those of rwtGTOV at each time point.

ACKNOWLEDGMENTS

We thank Thomas G. Ksiazek for providing the GTOV strain S-26764 and Mary Louise Milazzo for providing the isolation information of GTOV strain S-26764.

This research was funded by the National Institutes of Health/National Institute of Allergy and Infectious Diseases (U01AI151801 and K99AI156012) and John S. Dunn Foundation. Cheng Huang was supported in part by Public Health Service grant 1R21AI166985.

AUTHOR AFFILIATIONS

[1]Department of Pathology, University of Texas Medical Branch, Galveston, Texas, USA
[2]Department of Virology I, National Institute of Infectious Diseases, Shinjuku-ku, Tokyo, Japan
[3]Department of Microbiology and Immunology, University of Texas Medical Branch, Galveston, Texas, USA

AUTHOR ORCIDs

Satoshi Taniguchi http://orcid.org/0000-0002-2066-1979
Junki Maruyama http://orcid.org/0000-0003-0088-4793
Rachel A. Reyna http://orcid.org/0000-0001-8421-8397
Cheng Huang http://orcid.org/0000-0001-5402-353X
Masayuki Saijo https://orcid.org/0000-0001-5458-7298
Slobodan Paessler http://orcid.org/0000-0002-2213-9551

FUNDING

Funder	Grant(s)	Author(s)
HHS | NIH | National Institute of Allergy and Infectious Diseases (NIAID)	U01AI151801	Slobodan Paessler
HHS | NIH | National Institute of Allergy and Infectious Diseases (NIAID)	K99AI156012	Junki Maruyama
John S. Dunn Foundation (Dunn Foundation)		Slobodan Paessler
HHS | U.S. Public Health Service (PHS)	1R21AI166985	Cheng Huang

AUTHOR CONTRIBUTIONS

Satoshi Taniguchi, Conceptualization, Data curation, Formal analysis, Investigation, Methodology, Validation, Writing – original draft | Junki Maruyama, Funding acquisition, Methodology, Resources, Writing – review and editing | Takeshi Saito, Investigation, Writing – review and editing | Kirsten Littlefield, Methodology, Writing – review and editing | Rachel A. Reyna, Data curation, Writing – review and editing | John T. Manning, Methodology, Resources | Cheng Huang, Funding acquisition, Methodology, Validation, Writing – review and editing | Masayuki Saijo, Supervision, Writing – review and editing | Slobodan Paessler, Conceptualization, Funding acquisition, Project administration, Resources, Supervision, Writing – review and editing

ETHICS APPROVAL

All laboratory work using infectious GTOV was conducted in Biosafety Level 4 (BSL-4) facilities in the Galveston National Laboratory (GNL) at the University of Texas Medical Branch (UTMB) in Galveston in accordance with institutional safety guidelines, National Institutes of Health (NIH) guidelines, and US federal law. GTOV reverse genetics work was performed in the GNL BSL-4 facility under UTMB Notification of Use (NOU#2021004).

ADDITIONAL FILES

The following material is available online.

Supplemental Material

Supplemental figure legend and tables (JVI01964-23-s0001.docx). Legend for Fig. S1; Tables S1 and S2.
Fig S1 (JVI01964-23-s0002.tiff). Representative plaque morphologies of GTOV strains.

REFERENCES

1. Silva-Ramos CR, Montoya-Ruíz C, Faccini-Martínez ÁA, Rodas JD. 2022. An updated review and current challenges of Guanarito virus infection, Venezuelan hemorrhagic fever. Arch Virol 167:1727–1738. https://doi.org/10.1007/s00705-022-05453-3
2. Salas R, de Manzione N, Tesh RB, Rico-Hesse R, Shope RE, Betancourt A, Godoy O, Bruzual R, Pacheco ME, Ramos B. 1991. Venezuelan haemorrhagic fever. Lancet 338:1033–1036. https://doi.org/10.1016/0140-6736(91)91899-6
3. Fulhorst CF, Cajimat MNB, Milazzo ML, Paredes H, de Manzione NMC, Salas RA, Rollin PE, Ksiazek TG. 2008. Genetic diversity between and within the Arenavirus species indigenous to Western Venezuela. Virology 378:205–213. https://doi.org/10.1016/j.virol.2008.05.014
4. de Manzione N, Salas RA, Paredes H, Godoy O, Rojas L, Araoz F, Fulhorst CF, Ksiazek TG, Mills JN, Ellis BA, Peters CJ, Tesh RB. 1998. Venezuelan hemorrhagic fever: clinical and epidemiological studies of 165 cases. Clin Infect Dis 26:308–313. https://doi.org/10.1086/516299
5. Rodríguez-Morales AJ, Bonilla-Aldana DK, Risquez A, Paniz-Mondolfi A, Suárez JA. 2021. Should we be concerned about Venezuelan hemorrhagic fever? - a reflection on its current situation in Venezuela and potential impact in Latin America amid the migration crisis. New Microbes New Infect 44:100945. https://doi.org/10.1016/j.nmni.2021.100945
6. Radoshitzky SR, Buchmeier MJ, Charrel RN, Gonzalez J-PJ, Günther S, Hepojoki J, Kuhn JH, Lukashevich IS, Romanowski V, Salvato MS, Sironi M, Stenglein MD, Torre JC de la. 2023. ICTV virus taxonomy profile: Arenaviridae 2023. J Gen Virol 104. https://doi.org/10.1099/jgv.0.001891
7. Hallam SJ, Koma T, Maruyama J, Paessler S. 2018. Review of mammarenavirus biology and replication. Front Microbiol 9:1751. https://doi.org/10.3389/fmicb.2018.01751
8. Enria DA, Barrera Oro JG. 2002. Junin virus vaccines. Curr Top Microbiol Immunol 263:239–261. https://doi.org/10.1007/978-3-642-56055-2_12
9. Salam AP, Duvignaud A, Jaspard M, Malvy D, Carroll M, Tarning J, Olliaro PL, Horby PW. 2022. Ribavirin for treating lassa fever: a systematic review of pre-clinical studies and implications for human dosing. PLoS Negl Trop Dis 16:e0010289. https://doi.org/10.1371/journal.pntd.0010289

10. Okogbenin S, Erameh C, Okoeguale J, Edeawe O, Ekuaze E, Iraoyah K, Agho J, Groger M, Kreuels B, Oestereich L, Babatunde FO, Akhideno P, Günther S, Ramharter M, Omansen T. 2022. Two cases of Lassa fever successfully treated with ribavirin and adjunct dexamethasone for concomitant infections. Emerg Infect Dis 28:2060–2063. https://doi.org/10.3201/eid2810.220625
11. Huggins JW. 1989. Prospects for treatment of viral hemorrhagic fevers with ribavirin, a broad-spectrum antiviral drug. Rev Infect Dis 11:S750–61. https://doi.org/10.1093/clinids/11.supplement_4.s750
12. Enria DA, Briggiler AM, Sánchez Z. 2008. Treatment of Argentine hemorrhagic fever. Antiviral Res. 78:132–139. https://doi.org/10.1016/j.antiviral.2007.10.010
13. Veliziotis I, Roman A, Martiny D, Schuldt G, Claus M, Dauby N, Van den Wijngaert S, Martin C, Nasreddine R, Perandones C, Mahieu R, Swaan C, Van Praet S, Konopnicki D, Morales MA, Malvy D, Stevens E, Dechamps P, Vlieghe E, Vandenberg O, Günther S, Gérard M. 2020. Clinical management of Argentine hemorrhagic fever using ribavirin and favipiravir. Emerg Infect Dis 26:1562–1566. https://doi.org/10.3201/eid2607.200275
14. RadoshitzkySR, BuchmeierMJ, TorreJ-C. 2023. Arenaviridae: the viruses and their replication, p 784–809. In Knipe DM, Howley PM (ed), Fields Virology. Vol. 1. Lippincott Williams & Wilkins, Philadelphia, USA.
15. Gonzalez JP, Sanchez A, Rico-Hesse R. 1995. Molecular phylogeny of Guanarito virus, an emerging arenavirus affecting humans. Am J Trop Med Hyg 53:1–6.
16. Fehling SK, Lennartz F, Strecker T. 2012. Multifunctional nature of the arenavirus RING finger protein Z. Viruses 4:2973–3011. https://doi.org/10.3390/v4112973
17. Weaver SC, Salas RA, de Manzione N, Fulhorst CF, Duno G, Utrera A, Mills JN, Ksiazek TG, Tovar D, Tesh RB. 2000. Guanarito virus (Arenaviridae) isolates from endemic and outlying localities in Venezuela: sequence comparisons among and within strains isolated from Venezuelan hemorrhagic fever patients and rodents. Virology 266:189–195. https://doi.org/10.1006/viro.1999.0067
18. Ambrosio A, Saavedra M, Mariani M, Gamboa G, Maiza A. 2011. Argentine hemorrhagic fever vaccines. Hum Vaccin 7:694–700. https://doi.org/10.4161/hv.7.6.15198
19. Caplen H, Peters CJ, Bishop DH. 1985. Mutagen-directed attenuation of Rift Valley fever virus as a method for vaccine development. J Gen Virol 66 (Pt 10):2271–2277. https://doi.org/10.1099/0022-1317-66-10-2271
20. Alevizatos AC, McKinney RW, Feigin RD. 1967. Live, attenuated Venezuelan equine encephalomyelitis virus vaccine. Am J Trop Med Hyg 16:762–768.
21. Theiler M, Smith HH. 1937. The effect of prolonged cultivation *in vitro* upon the pathogenicity of yellow fever virus. J Exp Med 65:767–786. https://doi.org/10.1084/jem.65.6.767
22. Hansen CA, Barrett ADT. 2021. The present and future of yellow fever vaccines. Pharmaceuticals (Basel) 14:891. https://doi.org/10.3390/ph14090891
23. Zhang X, Wang Z, Ge S, Zuo Y, Lu H, Lv Y, Han N, Cai Y, Wu X, Wang Z. 2023. Attenuated African swine fever virus through serial passaging of viruses in cell culture: a brief review on the knowledge gathered during 60 years of research. Virus Genes 59:13–24. https://doi.org/10.1007/s11262-022-01939-z
24. Aw DZH, Heng KK, Heok JYH, Kong XY, Chen H, Zhang T, Zhai W, Chow VTK. 2022. Serial passaging of seasonal H3N2 influenza A/Singapore/G2-31.1/2014 virus in MDCK-SIAT1 cells and primary chick embryo cells generates HA D457G mutation and other variants in HA, NA, PB1, PB1-F2, and NS1. Int J Mol Sci 23:12408. https://doi.org/10.3390/-ijms232012408
25. Taniguchi S, Fukuma A, Tani H, Fukushi S, Saijo M, Shimojima M. 2017. A neutralization assay with a severe fever with thrombocytopenia syndrome virus strain that makes plaques in inoculated cells. J Virol Methods 244:4–10. https://doi.org/10.1016/j.jviromet.2017.01.005
26. Martínez-Sobrido L, Paessler S, de la Torre JC. 2017. Lassa virus reverse genetics. Methods Mol Biol 1602:185–204. https://doi.org/10.1007/978-1-4939-6964-7_13
27. Albariño CG, Bergeron E, Erickson BR, Khristova ML, Rollin PE, Nichol ST. 2009. Efficient reverse genetics generation of infectious Junin viruses differing in glycoprotein processing. J Virol 83:5606–5614. https://doi.org/10.1128/JVI.00276-09
28. Emonet SF, Seregin AV, Yun NE, Poussard AL, Walker AG, de la Torre JC, Paessler S. 2011. Rescue from cloned cDNAs and *in vivo* characterization of recombinant pathogenic Romero and live-attenuated candid #1 strains of Junin virus, the causative agent of Argentine hemorrhagic fever disease. J Virol 85:1473–1483. https://doi.org/10.1128/JVI.02102-10
29. Patterson M, Seregin A, Huang C, Kolokoltsova O, Smith J, Miller M, Smith J, Yun N, Poussard A, Grant A, Tigabu B, Walker A, Paessler S. 2014. Rescue of a recombinant Machupo virus from cloned cDNAs and *in vivo* characterization in interferon (alphabeta/gamma) receptor double knockout mice. J Virol 88:1914–1923. https://doi.org/10.1128/JVI.02925-13
30. Xu X, Peng R, Peng Q, Wang M, Xu Y, Liu S, Tian X, Deng H, Tong Y, Hu X, Zhong J, Wang P, Qi J, Gao GF, Shi Y. 2021. Cryo-EM structures of Lassa and Machupo virus polymerases complexed with cognate regulatory Z proteins identify targets for antivirals. Nat Microbiol 6:921–931. https://doi.org/10.1038/s41564-021-00916-w
31. Kang H, Cong J, Wang C, Ji W, Xin Y, Qian Y, Li X, Chen Y, Rao Z. 2021. Structural basis for recognition and regulation of arenavirus polymerase L by Z protein. Nat Commun 12:4134. https://doi.org/10.1038/s41467-021-24458-1
32. Ma J, Zhang S, Zhang X. 2021. Structure of Machupo virus polymerase in complex with matrix protein Z. Nat Commun 12:6163. https://doi.org/10.1038/s41467-021-26432-3
33. Barrett PN, Mundt W, Kistner O, Howard MK. 2009. Vero cell platform in vaccine production: moving towards cell culture-based viral vaccines. Expert Rev Vaccines 8:607–618. https://doi.org/10.1586/erv.09.19
34. Tong X, Smith J, Bukreyeva N, Koma T, Manning JT, Kalkeri R, Kwong AD, Paessler S. 2018. Merimepodib, an IMPDH inhibitor, suppresses replication of Zika virus and other emerging viral pathogens. Antiviral Res 149:34–40. https://doi.org/10.1016/j.antiviral.2017.11.004
35. Flatz L, Bergthaler A, de la Torre JC, Pinschewer DD. 2006. Recovery of an arenavirus entirely from RNA polymerase I/II-driven cDNA. Proc Natl Acad Sci U S A 103:4663–4668. https://doi.org/10.1073/pnas.0600652103
36. Sanger F, Nicklen S, Coulson AR. 1977. DNA sequencing with chain-terminating inhibitors. Proc Natl Acad Sci U S A 74:5463–5467. https://doi.org/10.1073/pnas.74.12.5463
37. Schmittgen TD, Livak KJ. 2008. Analyzing real-time PCR data by the comparative C(T) method. Nat Protoc 3:1101–1108. https://doi.org/10.1038/nprot.2008.73
38. Taniguchi S, Yoshikawa T, Shimojima M, Fukushi S, Kurosu T, Tani H, Fukuma A, Kato F, Nakayama E, Maeki T, Tajima S, Lim CK, Ebihara H, Kyuwa S, Morikawa S, Saijo M. 2020. Analysis of the function of the lymphocytic choriomeningitis virus S segment untranslated region on growth capacity *in vitro* and on virulence *in vivo*. Viruses 12:896. https://doi.org/10.3390/v12080896